PHYSICAL REVIEW B VOLUME 15, NUMBER 10 15 MAY 1977

Two-photon photoemission from metals induced by picosecond laser pulses*

J. H. Bechtel,† W. Lee Smith,‡ and N. Bloembergen
Gordon McKay Laboratory, Harvard University, Cambridge, Massachusetts 02138
(Received 30 September 1976)

We have measured the two-photon photoemission current density from tungsten, tantalum, and molybdenum when irradiated by 532-nm wavelength radiation. This wavelength was produced by the second-harmonic radiation of single picosecond laser pulses from a mode-locked neodymium-doped yttrium-aluminum-garnet laser. The results are interpreted in terms of both a simple temperature-independent two-photon photoemission effect and a generalization of the Fowler-DuBridge theory of photoemission. The laser polarization dependence of the emitted current is also reported.

I. INTRODUCTION

Since the development of the laser there have been numerous experiments that have reported electron emission from solid targets irradiated by high-power laser pulses.[1-3] These results have usually been interpreted as due to either thermionic emission produced by the laser-induced temperature rise at the irradiated surface or to a photoemission effect. For sufficiently strong electromagnetic fields that accompany the laser pulse, these photoemission effects may be either a single-photon process or a multiple-photon process.

The earliest laser-induced electron emission experiments[4] reported that burst mode lasers could produce substantial electron emission from metal targets. These experiments were all interpreted as thermionic emission induced by the heating action of the laser. Unfortunately, the complicated temporal structure of the relaxation oscillations in the burst mode laser made it difficult to perform a detailed study of the electron emission process.

Ready[5] reported laser-induced electron emission produced by Q-switched ruby-laser pulses with a peak irradiance in the range of 10–25 MW/cm^2 and approximately 50-nsec pulse width (full width at half-maximum). He concluded that the observed electron emission was explainable as thermionic emission, and data were reported for tungsten, thoriated tungsten, and platinum target materials.

In other experiments lasers have been used to study electron emission that was inferred to be other than thermionic. Teich and Wolga[6] used a pulsed GaAs laser to study two-photon photoemission from sodium. Logothetis and Hartman[7] studied both two-photon and three-photon photoemission from gold and stainless steel by the use of a ruby laser and its second-harmonic radiation.

The observation of multiple-photon photoemission has more recently been facilitated by the use of high-power, ultrashort pulse, mode-locked lasers. These lasers can produce the very high irradiance necessary for the observation of multiple-photon photemission, and because of the very short pulse duration, thermal electron emission effects may often be avoided. Preliminary results of electron emission produced by a mode-locked neodymium-doped glass laser have been presented in Ref. 8. Unfortunately, these results were inconclusive because the entire pulse train of the mode-locked laser was used, and an asymmetry of the electron emission was observed depending upon whether it was produced by the leading or the trailing portions of the pulse train. Additional experiments[9] attributed this asymmetry in part to pulse distortion in the trailing portion of the train of the pulses.

In 1975 we reported experiments on laser-induced electron emission produced by single picosecond pulses switched from the train of a mode-locked YAlG:Nd (neodymium-doped yttrium-aluminum-garnet) laser.[10] Other experiments utilizing single picosecond pulses have also recently been reported.[11]

In the experiments reported here we extend our previous results to other materials besides tungsten. In addition, we report data for electron emission from metals using the second-harmonic radiation from a mode-locked YAlG:Nd laser. Moreover, we have increased the sensitivity of the electron detection system by utilizing an electron multiplier.

In Sec. II we outline theories of both pure multiple-photon photoemission and multiple-photon photoemission combined with thermal emission mechanisms. In Sec. III the experimental apparatus and procedure are discussed. In Sec. IV the results of the electron emission measurements are

presented. Finally, in Sec. V we discuss the results of our experiments and their relation to other experiments and theory.

II. THEORY

A. Multiquantum photoemissive effect in metals without heating

We shall first consider the case of multiple-photon photoemission from a metal at a temperature $T=0\,^{\circ}\mathrm{K}$. The calculations of pure multiple-photon photoemission have been either for the so-called surface photoemission effect or for the volume photoemission effect. The initial calculations for the two-photon surface photoemission effect were done by Makinson and Buckingham,[12] R. L. Smith,[13] and Adawi.[14] Calculations of higher order multiple-photon photoemission effects have been given by Bunkin and Fedorov[15] and by Silin.[16]

A theoretical treatment of the two-photon volume photoemissive effect was first given by Bloch.[17] Bloch's calculation has been criticized by Teich and Wolga,[6] who observed that Bloch failed to account for the following: (i) the electron escape depth is a function of the electron energy, (ii) part of the incident light is reflected at the surface, (iii) the perturbation Hamiltonian in the independent electron scheme is $H=-e\vec{A}\cdot\vec{p}/mc+e^2A^2/2mc^2$, and two-photon transitions may occur from either the first term in second order or from the second term in first order. Bloch neglected the first term. Teich and Wolga obtained an explicit relation for the two-photon photoemission current and found that their calculation was in good agreement with their experimental results of sodium irradiated by a gallium-arsenide laser. Logothetis and Hartman[7] used a similar multiquantum volume photoemission model to explain their experiments on gold.

As an example, consider two-photon photoemission. In this case the two-photon induced current density, J_2 is given by the expression

$$J_2=ep\int_0^{\infty}\frac{I}{h\nu}(1-R)\beta_{pe}I(1-R)e^{-x/l}e^{-2\alpha x}\,dx$$

$$=\frac{epI^2(1-R)^2\beta_{pe}}{h\nu(2\alpha+1/l)}\,. \tag{1}$$

Here e is the electron charge, p is the electron escape probability, R is the metal reflectivity, I is the incident power per unit area, $h\nu$ is the incident photon energy, α is the absorption coefficient at the laser wavelength, and l is the electron escape depth. The total TPA (two-photon absorption) coefficient may be written as

$$\beta=\beta_{pe}+\beta_c \tag{2}$$

with β_c the TPA coefficient for transitions ending below the vacuum level. The parameter β_{pe} is the TPA coefficient that results in photoemissive transitions.

By similar arguments one can easily construct expressions for higher-order multiple-photon photoemissive current densities.

B. Generalized Fowler-DuBridge theory

The first theory to successfully explain both the temperature dependence of one-photon photoemission and the spectral dependence of one-photon photoemission near the work-function threshold was developed by Fowler.[18] Fowler's starting point is the assumption that the electrons in the metal obey Fermi-Dirac statistics and are uniformly distributed in momentum space. He calculated the one-photon quantum yield for three different models that depended on how the photon was absorbed and how the electron escaped. Shortly thereafter DuBridge[19] extended Fowler's calculations using slightly different assumptions for both the photon absorption and the electron emission, and he calculated the one-photon quantum yield as a function of temperature and one-photon energy.

These ideas of Fowler and DuBridge may easily be extended to more general electron emission effects.[20] Our basic tenet is that the total electron emission current density is composed of partial current densities each of which has a simple interpretation. Thus we write the total current density as

$$\vec{J}(\vec{r},t)=\sum_{n=0}^{\infty}\vec{J}_n(\vec{r},t)\,. \tag{3}$$

The quantity J_0 is interpreted as thermionic emission, J_1 as one-photon photoemission, and J_n as n-photon photoemission. In order to derive the functional form of the partial current density for n-photon photoemission, we adopt assumptions similar to those of DuBridge.[19] This result for the n-photon current density is

$$|\vec{J}_n(\vec{r},t)|=a_n(e/h\nu)^nA\,I(\vec{r},t)^n(1-R)^n$$

$$\times T(\vec{r},t)^2F\left(\frac{nh\nu-\phi}{kT(\vec{r},t)}\right). \tag{4}$$

Here e is the electron charge, R is the surface reflectivity, A is the theoretical Richardson coefficient ($120\ \mathrm{A/cm^2\,^{\circ}K^2}$), $h\nu$ is the laser photon energy, ϕ is the surface work function, k is Boltzmann's constant, I is the incident laser irradiance, T is the absolute temperature of the surface, and a_n is a constant. The function $F(x)$ is the Fowler function and is plotted in Fig. 1.

A comparison of Eq. (1) and Eq. (4) shows that the constant a_2 can be related to the escape pro-

bability p, the two-photon absorption coefficient β_{pe}, and other atomic constants by the relation

$$a_2 = \frac{p\beta_{pe}h^4\nu}{2\pi m e^2(2\alpha + 1/l)(2h\nu - \phi)^2} . \quad (5)$$

On the other hand, the constant a_2 can also be related to the measured emitted charge q if the electron emission is a pure two-photon effect. In this interpretation a_2 is a completely empirical parameter and is found by choosing a_2 such that the measured charge is equal to the theoretical expression for the emitted charge, i.e.,

$$q = \int \vec{J}(\vec{r}, t) \cdot d\vec{S}\, dt . \quad (6)$$

The integration is to be taken over the pulse duration and the pulse area. The total current density $\vec{J}(\vec{r}, t)$ is given by Eqs. (3) and (4) if both the space-time dependence of the incident laser irradiance and the surface temperature are known. The irradiance is usually known from the experimentally measured laser diagnostics, but the surface temperature as a function of space and time must be calculated from the heat-conduction equation. This equation is

$$\nabla^2 T(\vec{r}, t) - \frac{1}{\kappa}\frac{\partial T(\vec{r}, t)}{\partial t} = -\frac{G(\vec{r}, t)}{K} . \quad (7)$$

Here κ is the thermal diffusivity, K is the thermal conductivity, and $G(\vec{r}, t)$ is the net energy generated per unit volume per unit time within the metal. The solution to Eq. (7) and the application of this solution to picosecond laser pulses has recently been given by one of us and will not be repeated here.[21]

Finally, we should mention that it has recently been suggested that very short laser pulses should lead to anomalous heating of metals in which the electrons and the lattice are not in thermal equilibrium on the time scale of the laser pulse.[22] We have calculated the expected electron temperature by the technique of Ref. 22, and we find that there is no significant difference between this calculation and those based on the techniques of Ref. 21 for laser pulse durations of tens of picoseconds, as used in this experiment. Thus the more simple methods (e.g., Ref. 21) of calculating the surface temperature are adequate.

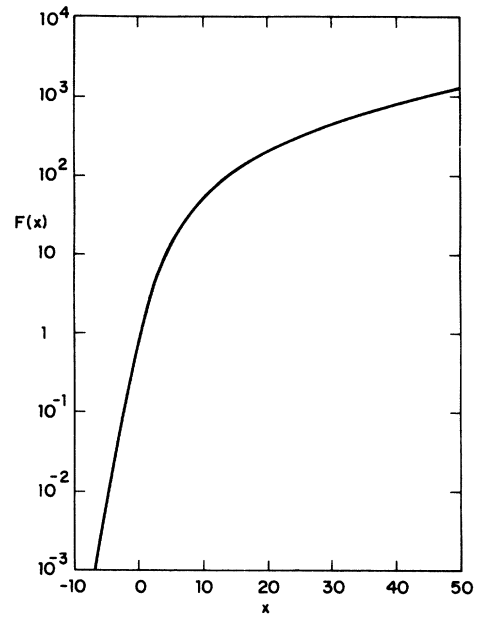

FIG. 1. Fowler function $F(x)$.

III. EXPERIMENTAL APPARATUS AND TECHNIQUES

A. Laser system

A passively mode-locked YAlG:Nd laser system produced the picosecond pulses used in these experiments. A schematic diagram of the experimental apparatus is exhibited in Fig. 2. The laser oscillator is a xenon flashlamp pumped 6-mm diam by 7.62-cm long YAlG:Nd rod in the Brewster-Brewster configuration. This oscillator is simultaneously Q switched and mode locked by a flowing saturable absorber (Kodak 9860) in contact with the high-reflectivity mirror of the oscillator cavity. The output of the oscillator is limited to the TEM_{00} mode by a 2-mm diam intracavity aperture. The time dependence of the oscillator output consists of a sequence of picosecond pulses separated by

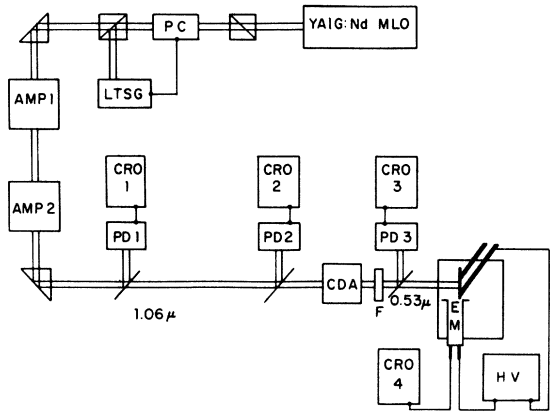

FIG. 2. Schematic diagram of the experimental apparatus. YAlG:Nd MLO, neodymium-doped yttrium-aluminum-garnet mode-locked laser oscillator; PC, Pockels cell; LTSG, laser-triggered spark gap; AMP, neodymium-doped yttrium-aluminum-garnet laser amplifier; CRO, oscilloscope; PD, photodiode; CDA, cesium-dihydrogen-arsenate frequency doubler; F, filter; EM, electron multiplier; HV, high-voltage power supply.

approximately 8 nsec. From this sequence of pulses a single pulse is selected by a cylindrical-ring-electrode potassium dideuterium phosphate Pockels cell. This Pockels cell is positioned between crossed Glan prisms, and is activated by a laser-triggered spark gap. The selected laser pulse is subsequently amplified by two YAlG:Nd laser amplifiers.

A high-speed biplanar photodiode PD-1 (ITT F4000) is used in conjunction with CRO-1, a Tektronix 519 oscilloscope, to insure that only a single pulse is selected from the oscillator train of pulses. A calibrated photodiode PD-2 (S-1 response) measures the energy of the pulse at 1.064-μm wavelength.

In order to produce 2.33-eV picosecond pulses, the single picosecond 1.165-eV pulses are subsequently frequency doubled by allowing these infrared pulses to traverse a 90° phase-matched CDA (cesium dihydrogen arsenate) crystal. This crystal orientation is such that the input laser beam is perpendicular to the optic axis and at 45° to the crystal X and Y axes. The temperature required for the 90° phase matching is approximately 42 °C. This temperature is maintained during the experiment by a temperature probing thermistor connected to a proportional temperature controller.

The output radiation from the CDA crystal is subsequently filtered to remove all remaining 1.064-μm radiation, and the energy of the pulse at wavelength 0.532 μm is measured with a calibrated photodiode PD-3 (S-20 response).

B. Pulse characteristics

For an accurate quantitative measurement of many nonlinear optical properties of materials it is necessary to know the spatial and temporal form of the pulse incident on the material being studied. The spatial profile of the 0.532-μm laser pulse incident on the metal surfaces was determined at the site of the metal target by using an oscilloscope coupled to the output of a linear array of 256 silicon photodiodes. The center-to-center spacing between the photodiodes is 50.8 μm. The spatial profile of the incident laser pulse irradiance was found to be nearly Gaussian in form, and the pulse area was measured to be 4.52×10^{-2} cm^2.

Initially we attempted to perform some of these experiments with a KDP (potassium dihydrogen phosphate) crystal instead of the CDA doubling crystal. The angle-tuned phase matching KDP crystal exhibited, however, significant pulse distortion as measured with the photodiode array. Presumably this distortion was due to both mechanical instabilities in the apparatus holding the crystal and the walk-off problem[23] that is associated with angle-tuned phase matching.

In order to determine the temporal pulse duration, two techniques were used to measure the 1.064-μm pulse width. In the first technique, two-photon fluorescence photography, the initial pulse is split into two pulses by a beamsplitter. These pulses are redirected by mirrors to overlap within a two-photon absorbing material such as rhodamine 6G. The dye fluorescence is photographed, and the pulse duration is determined by the spatial distribution of the exposure produced by the fluorescence track. In the second method, second-harmonic autocorrelation, the pulse is split into two pulses by a Michelson interferometer. The two pulses are collinearly recombined after one pulse has been delayed by a variable amount. The recombined pulses are subsequently directed through a phase-matched second-harmonic generation crystal. One plots the second-harmonic signal as a function of delay. The results of both the two-photon fluorescence photography and the second-harmonic autocorrelation method give an average temporal duration full width at half maximum of 30 ± 6 psec for the 1.064-μm wavelength laser pulse.

For a temporally Gaussian laser pulse the second-harmonic signal will be a factor of 1.414 shorter, if the conversion efficiency is small.

To determine the maximum incident irradiance of an individual pulse, it is necessary to know the pulse energy, the pulse duration, the pulse area, and the pulse shape. The pulse energy at the second harmonic wavelength, $\mathcal{E}_{sh}$, is determined by the output of photodiode PD-3. A convenient way to measure the pulse irradiance for individual pulses is to employ a nonlinear optic technique.[24] This method was first suggested by Glenn and Brienza[25] and involves measuring both the incident pulse energy $\mathcal{E}_f$ at wavelength 1.064 μm and the total energy of the second harmonic pulse $\mathcal{E}_{sh}$. For small second-harmonic conversion efficiencies the ratio $\mathcal{E}_f^2/\mathcal{E}_{sh}$ is proportional to the product of the pulse duration and the pulse area. We thus normalized our data so that the average low incident irradiance pulses produced an average pulse duration of 30 psec for the 1.064-μm wavelength or 21.2 psec for the 0.532-μm wavelength.

At the largest incident irradiances we noticed that the average value of $\mathcal{E}_f^2/\mathcal{E}_{sh}$ was larger than the corresponding expression at the lowest irradiances. Therefore, no doubt, the green pulse was somewhat distorted from its low conversion efficiency shape. However, by employing this nonlinear optic technique, an effective maximum irradiance is still measured, and gives a good approximation to the true maximum incident irradiance.

C. Vacuum system and electron multiplier

The vacuum system used for these electron emission measurements was a stainless-steel device. After the introduction of a new target material into the chamber, the initial atmospheric pressure was reduced to approximately 1 mTorr by the use of two liquid-nitrogen-cooled sorption pumps. This pressure was subsequently reduced to approximately 1×10^{-8} Torr by the use of an ion pump. A Bayard-Alpert ionization gauge monitored the residual pressure during the taking of data, and this pressure was always between 5×10^{-9} and 2×10^{-8} Torr.

The electron multiplier was mounted approximately 1 cm below the target cathode. The multiplier was an RCA C31019B, 14-stage, copper-beryllium dynode device. During the taking of data the total voltage across the dynodes was either 2000 or 3000 V. Since the anode of the multiplier was at ground potential, the entrance or focusing electrode of the multiplier was at a negative voltage. For adequate collection of electrons, therefore, the cathode or laser target electrode was maintained typically at 500 V negative with respect to the focusing electrode. Our initial experiments utilizing the third harmonic of the YAlG:Nd laser (3547 Å) incident on a calcium cathode allowed us not only to measure the absolute gain of the electron multiplier at different voltages but also to test the electron multiplier for space charge linearity. Since 3547-Å radiation on Ca produces a one-photon photoemission effect, this particular arrangement allows us to test the linearity of the electron multiplier with incident electron pulses of approximately the temporal duration as those in the multiphoton photoemission experiments.

During the taking of data the gain of the electron multiplier was always adjusted so that the electron multiplier was operating in the linear region.

A copper shield with holes for passage of the laser pulse was placed around the target cathode and the focusing electrode of the electron multiplier. This shield was maintained at the cathode voltage to insure that a significant fraction of the emitted electrons impinged on the first dynode. Without the shield the current was more than an order of magnitude less, and most of the emitted electrons were collected by the metallic vacuum chamber walls that were at ground potential.

D. Procedure

The technique for measuring the electron emission was to measure the total emitted charge from the cathode for each single-laser pulse. This was determined by electronically integrating the current pulse and measuring the voltage produced by this circuit on an oscilloscope. We also determined the maximum incident irradiance by the method outlined in Sec. III B. The data were plotted as the maximum current density versus the maximum incident irradiance. The maximum current density J_{max} was computed from the total emitted charge q using the expression $J_{max}=2\sqrt{2}q/\pi^{3/2}\tau d^2$. Here τ is the $1/e$ pulse half-width, and d is the $1/e$ intensity radius of the incident spatially and temporally Gaussian pulse. Except for those experiments dealing with the laser polarization dependence of the emitted current, the laser was incident normal to the target electrode to within $\pm5°$.

Finally, we should note that before each experiment was started, we outgassed the target cathode. This was accomplished by passing a low-voltage ac current through the 254-μm thick ribbon electrode. Since all of the elements that we studied are refractory metals, they have very high melting points. We were thus able to bring the surfaces to temperatures greater than 2000 °C for several minutes just prior to the taking of photoemission data.

IV. EXPERIMENTAL RESULTS

We have observed two-photon photoemission from tantalum, molybdenum, and tungsten targets irradiated by single laser pulses of wavelength 5321 Å. An example of the two-photon photoemission from Ta is exhibited in Fig. 3.

When the maximum emitted current density is plotted versus the maximum incident irradiance on log-log graph paper, the data are approximately a straight line with slope two.

The maximum current density J_{max} may be expressed as $J_{max}=bI_{max}^2$, where I_{max} is the incident maximum irradiance. The experimentally determined value of the coefficient b is given in Table I. This value is related to a_2 for each element, which is also given in Table I. The value of a_2 was chosen so that the experimentally measured charge was equal to the computed charge by numerical integration of Eq. (6) with J_2 substituted from Eq. (4). The value of a_2 for a given material, as inferred from our experiments, depends on the work function of the material in question. Therefore the values of the work functions that we assumed are also listed in Table I.

The polarization dependence of the two-photon photoemission was also investigated in our experiments. We studied the element tantalum using a laser radiation angle of incidence of 45°. We observed that the current density for an incident p-wave polarization is 3.2 times larger than the

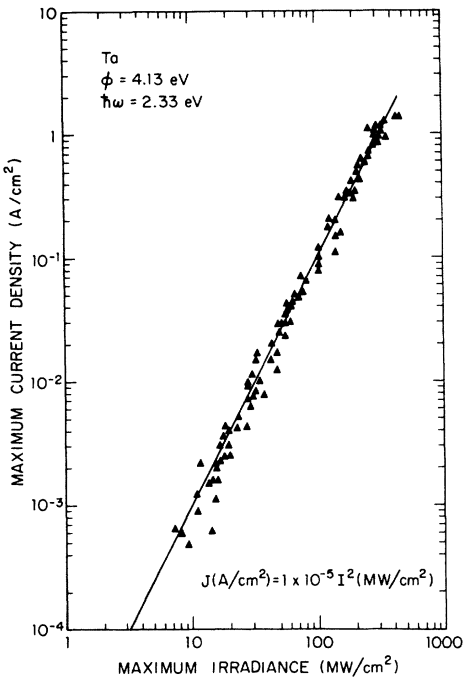

FIG. 3. Two-photon photoemission maximum current density plotted against maximum incident irradiance for the element tantalum. The work function of Ta is 4.13 eV, and the incident photon energy is 2.33 eV.

current density for an s-wave polarization if the s wave and p wave have the same irradiance.

V. DISCUSSION AND SUMMARY

We have demonstrated two-photon photoemission from Ta, Mo, and W using ultrashort laser pulses of wavelength 5321 Å. The functional relation between the maximum emitted current density J_{max} and the maximum incident irradiance I_{max} obeys the relation $J_{max} = bI^2_{max}$. The coefficient b was determined for these three elements. It is interesting to compare our values of this coefficient with those available from the literature. There are only two other measurements that are known, $b = 8 \times 10^{-4}$ A cm^2/MW^2 for Na,[6] and $b = 2.4 \times 10^{-3}$ A cm^2/MW^2 for Au.[7] Our values of b are thus several orders of magnitude smaller than the previously measured values.

TABLE I. Materials, work functions, and two-photon parameters for this experiment.

Material	ϕ(eV)	b (A cm^2/MW^2)	a_2 (cm^4/A^2)
Ta	4.13[a]	1×10^{-5}	9.3×10^{-26}
Mo	4.41[b]	6×10^{-7}	2.5×10^{-26}
W	4.49[c]	5×10^{-7}	2.6×10^{-26}

[a] J. L. Gumnick and D. W. Juenker, J. Appl. Phys. 31, 102 (1960).
[b] R. C. Jaklevic and D. W. Juenker, J. Appl. Phys. 33, 562 (1962).
[c] L. Apker, E. Taft, and J. Dickey, Phys. Rev. 73, 46 (1948).

It is of more interest to interpret our experimental results using a model that is a generalization of the Fowler-DuBridge model. This model includes the temperature effects associated with the laser-induced temperature rise as well as the laser frequency and work function dependence. For our experiments on two-photon photoemission, only the contribution J_2 contributes to the partial current densities of Eq. (3). The value of a_2 is chosen so that the experimentally measured charge is equal to the theoretically computed charge using Eq. (6) and Eq. (4) for J_2. This integration was done numerically on a digital computer and exploited the laser-induced temperature changes as given in Ref. 21. We should note that in principle we should be able to calculate a_2 from Eq. (5), since a_2 is related to the atomistic parameters of this relation. Unfortunately, the uncertainties in the escape probability, the escape depth, and the two-photon absorption coefficient are large, and no accurate calculation of a_2 is presently possible.

The polarization dependence of the current density is also very interesting. The theories of surface two-photon photoemission[12-16] predict no two-photon photoemission for an s-wave incident polarization. Our experiments, therefore, support the view that two-photon photoemission is, in part, volume in nature. This conclusion is in agreement with the viewpoint of Refs. 6 and 7.

*Supported by the Joint Services Electronics Program and NASA.
†Present address: General Motors Research Laboratories, Warren, Mich. 48090.
‡Present address: Lawrence Livermore Laboratory, Livermore, Calif. 94550.

[1] J. F. Ready, *Effects of High Power Laser Radiation* (Academic, New York, 1971), Chap. 4, p. 127.
[2] A. D. Gladun and P. P. Barashev, Usp. Fiz. Nauk 98, 493 (1969) [Sov. Phys.-Usp. 12, 490 (1970)].

[3]P. P. Barashev, Phys. Status Solidi A 9, 9 (1972).
[4]D. Lichtman and J. F. Ready, Phys. Rev. Lett. 10, 342 (1963); R. E. Honig and J. R. Woolston, Appl. Phys. Lett. 2, 138 (1963); C. M. Verber and A. H. Adelman, *ibid.* 2, 220 (1963); F. Giori, L. A. MacKenzie, and E. J. McKinney, *ibid.* 3, 25 (1963).
[5]J. F. Ready, Phys. Rev. 137, A620 (1965).
[6]M. C. Teich and G. J. Wolga, Phys. Rev. 171, 809 (1968).
[7]E. M. Logothetis and P. L. Hartman, Phys. Rev. 187, 460 (1969).
[8]Gy. Farkas, Z. Gy. Horvath, I. Kertesz, and G. Kiss, Nuovo Cimento Lett. 1, 314 (1971).
[9]Gy. Farkas and Z. Gy. Horvath, Opt. Commun. 12, 392 (1974).
[10]J. H. Bechtel, W. L. Smith, and N. Bloembergen, Opt. Commun. 13, 56 (1975).
[11]L. A. Lompre, J. Thebault, and Gy. Farkas, Appl. Phys. Lett. 27, 110 (1975).
[12]R. E. B. Makinson and M. J. Buckingham, Proc. Phys. Soc. Lond. A 64, 135 (1951).
[13]R. L. Smith, Phys. Rev. 128, 2225 (1962).
[14]I. Adawi, Phys. Rev. 134, A788 (1964).
[15]F. V. Bunkin and M. V. Fedorov, Zh. Eksp. Teor. Fiz. 48, 1341 (1965) [Sov. Phys.-JETP 21, 896 (1965)].
[16]A. P. Silin, Fiz. Tverd. Tela 12, 3553 (1970) [Sov. Phys.-Solid State 12, 2886 (1971)].
[17]P. Bloch, J. Appl. Phys. 35, 2052 (1964).
[18]R. H. Fowler, Phys. Rev. 38, 45 (1931).
[19]L. A. DuBridge, Phys. Rev. 43, 727 (1933).
[20]J. H. Bechtel, Ph.D. thesis (University of Michigan, 1973) (unpublished).
[21]J. H. Bechtel, J. Appl. Phys. 46, 1585 (1975).
[22]S. I. Anisimov, B. L. Kapelivich, and T. L. Perel'man, Zh. Eksp. Teor. Fiz. 66, 776 (1974) [Sov. Phys.-JETP 39, 375 (1974)].
[23]D. A. Kleinman, Phys. Rev. 128, 1761 (1962).
[24]W. L. Smith and J. H. Bechtel, J. Appl. Phys. 47, 1065 (1976).
[25]W. H. Glenn and M. J. Brienza, Appl. Phys. Lett. 10, 221 (1967).